J Appl Electrochem (2009) 39:55–64
DOI 10.1007/s10800-008-9636-x

ORIGINAL PAPER

Nickel-dimethylglyoxime complex modified graphite and carbon paste electrodes: preparation and catalytic activity towards methanol/ethanol oxidation

William S. Cardoso · Vera L. N. Dias · Wendell M. Costa · Isaide de Araujo Rodrigues · Edmar P. Marques · Antonio G. Sousa · J. Boaventura · Cicero W. B. Bezerra · Chaojie Song · Hansan Liu · Jiujun Zhang · Aldaléa L. B. Marques

Received: 10 March 2008 / Accepted: 8 July 2008 / Published online: 25 July 2008

Abstract Nickel-dimethylglyoxime complex (abbreviated as Ni(II)$(DMG)_2$) modified carbon paste and graphite electrodes were prepared by mixing Ni(II)$(DMG)_2$ with graphite paste, and coating Ni(II)$(DMG)_2$ to the graphite surface. It is necessary to cycle the electrode potential to a high value (e.g. 0.8 V versus SCE) for the preparation of the modified electrodes. The electrochemical reaction was originally assumed to be a one-electron process converting Ni(II)$(DMG)_2$ to $[(DMG)_2(H_2O)Ni(III)ONi(III)(OH)(DMG)_2]^-$. $[(DMG)_2(H_2O)Ni(III)ONi(III)(OH)(DMG)_2]^-$ showed a strong catalytic activity toward electro-oxidation of methanol and ethanol. The electrocatalytic oxidation currents consistently increase with the increase in Ni(II)$(DMG)_2$ loading, OH^-, and alcohol concentrations. Rotating disk electrode results obtained with a Ni(II)$(DMG)_2$ coated graphite disk electrode showed that the electrocatalytic oxidation of alcohol is a 4-electron process producing formate anion (methanol oxidation) or acetate anion (ethanol oxidation). A mechanism for the electrocatalytic oxidation of methanol/ethanol was proposed, and a rate-determining step was also discussed.

Keywords Ethanol · Methanol · Electro-oxidation · Electrocatalysts · Nickel-dimethylglyoxime · Carbon paste · Graphite electrodes

W. S. Cardoso · I. de Araujo Rodrigues · E. P. Marques · C. W. B. Bezerra
Department of Chemistry, Federal University of Maranhão, Av. dos Portugueses, S/N, Campus do Bacanga, São Luis, MA 65080-040, Brazil

V. L. N. Dias · W. M. Costa · A. L. B. Marques (✉)
Department of Technology Chemistry, Federal University of Maranhão, Av. dos Portugueses, S/N, Campus do Bacanga, São Luis, MA 65080-040, Brazil
e-mail: aldalea@quimica.ufma.br

A. G. Sousa
Department of Chemistry, Federal University of Paraiba, Cidade Universitaria, Joao Pessoa, PB 58051-970, Brazil

J. Boaventura
Institute of Chemistry, Federal University of Bahia, Barao de Jeremoado, S/N, Campus Universitario de, Ondina, Salvador, BA 40170-115, Brazil

C. Song · H. Liu · J. Zhang (✉)
Institute for Fuel Cell Innovation, National Research Council Canada, Vancouver, BC, Canada V6T 1W5
e-mail: jiujun.zhang@nrc.gc.ca

1 Introduction

Methanol and ethanol are important bio-fuels that can be generated from renewable bioresources. They have many industrial applications, especially in renewable energy technologies such as direct liquid fuel cells. However, the kinetics of electrochemical oxidation of these alcohols is slow. Efforts have been devoted to catalyst development for the electrooxidation of these alcohols. The most extensively investigated catalysts are Pt based catalysts including Pt, as well as both Pt transition metal binary and ternary alloys. These works have been reviewed by several authors recently [1–3]. Other noble metal based materials such as Pd based catalysts [4], and Ir based catalysts have also been studied [5]. However, the high cost and limited resources for these materials greatly restrict their application.

Nickel and nickel compounds have attracted interest in catalyzing electrooxidation of small organic molecules. Recently hollow nickel spheres have been used as catalysts for methanol and ethanol oxidation [6], and kinetic studies of ethanol oxidation on CuNi alloy supported PtRu and PtMo catalysts have also been investigated [7]. Nickel

oxide/hydroxides and nickel-tetraazamacrocyclic complexes are known to be capable of catalyzing alcohol oxidation in an alkaline medium. Taraszewska [8], El-Shafei [9], and Fleischmann et al. [10] have reported the electro-oxidation of methanol catalyzed by Ni hydroxide coated on glassy carbon electrodes or on Ni electrodes. NiOOH was found to be the active species responsible for the catalytic activity. This catalytic activity has been used in liquid chromatographic detection of aliphatic alcohols [11]. Ni complexes demonstrated higher catalytic activity than NiOOH. Roslonek and Taraszewska [12] and Bae et al. [13] investigated catalytic activity of Ni tetraaza macrocycle towards alcohol and L-ascorbic oxidations, and found that Ni tetraaza macrocyclic complexes showed lower overpotential (0.1 V lower) than NiOOH, and that the oxidation current is approximately five times higher than NiOOH. Nickel porphyrine-catalyzed methanol electro-oxidation has been reported by Golabi and Nozad [14], and Ciszewski and Milczarek [15]. Other nickel coordination compounds such as Ni-1-(2-pyridylazo)-naphthol have also been investigated [16].

Diamethyglyoxime is one of the most commonly used ligands coordinating nickel ions, which forms nickel-dimethyglyoxime complexes due to its sensitivity and stability. The ligand can adsorb on an electrode surface and significantly enhance the electrochemical response of Ni ions. This property has been used in the detection of Ni ions in natural water [17–19]. Most recently, the catalytic activity of the nickel-dimethylglyoxime complex towards the electro-oxidation of methanol has been reported [20, 21], where the catalytically active site is ascribed to NiOOH and the dimethylglyoxime ligand was not considered.

In earlier works, nickel hydroxide, or nickel complex, modified electrodes, were prepared usually by oxidizing nickel electrodes in an alkaline solution [10], running scans with the nickel rod in solutions which contain the ligand [20, 21], running scans with the working electrode in nickel complex alkaline solutions [12, 13, 15, 22, 23], deposit nickel salt solutions to the electrode surface followed by cycling it in alkaline solution [9, 11], alternate immersion of the working electrode in nickel salt and then alkaline solutions [8], or directly depositing nickel complex solutions onto the electrode surface [14]. Alternatively, modified electrodes were also prepared by consecutive deposition of nickel salt solution and ligand solution onto the electrode surface [16]. In all these methods, cycling the working electrode potential is required. However, how the cycling potential affects the formation of the modified electrode was not reported.

In this work, we prepared thinly layered $Ni(DMG)_2$ modified electrodes by using consecutive drop deposition of Ni salt and DMG solutions, followed by cycling the potential to a certain value. The effect of oxidation potential on the preparation of nickel-dimethylglyoxime was investigated. Carbon paste electrodes (CPEs) are popular because carbon pastes are easily obtained at minimal costs and CPEs can be easily prepared. However, Ni-dimethylglyoxime modified carbon paste electrodes have not yet been reported in literature. We also prepared 3-D Ni-dimethylglyoxime modified carbon paste electrodes by mixing the Ni-dimethylglyoxime complex with the graphite paste. These modified electrodes showed strong catalytic activity toward the ethanol/methanol oxidation.

2 Experimental

2.1 Reagents

Dimethylglyoxime ($CH_3C(=NOH)C(=NOH)CH_3$, abbreviated as DMG), nickel(II) sulphate, sodium hydroxide, and ethanol and methanol were obtained from Merck, and used as received. All aqueous solutions were prepared with doubly distilled water purified through a NANOPURE system. Bis-(dimethylglyoxime) nickel(II) complex (abbreviated as $Ni(II)(DMG)_2$)) was prepared according to a literature procedure [24]. Briefly, 50 mL of 0.02 mol L^{-1} DMG in an alcoholic solution were mixed with 50 mL of Ni(II) sulfate aqueous solution, immediately followed by the addition of 5 mL of 1.0 mol L^{-1} NaOH aqueous solution. The addition of OH^- anions was to facilitate the formation of $Ni(II)(DMG)_2$, a rose-red precipitate. The reaction of such a synthesis can be described as reaction (I):

$$\begin{aligned} &Ni(II) + 2CH_3C(=NOH)C(=NOH)CH_3 \\ &\rightarrow Ni(II)(CH_3C(=NO)C(=NOH)CH_3)_2 + 2H^+ \end{aligned} \quad (I)$$

This $Ni(II)(DMG)_2$ was filtered, exhaustively washed with deionized water, and then dried at room temperature. The product was characterized using a Bomen MB series infrared spectrophotometer. Pressed KBr pellets containing 1% (wt%) of the product were measured with a 4 cm^{-1} resolution and 50 cumulative scans. Figure 1 shows the infrared spectra of the reaction precursor dimethylglyoxime and the reaction product ($Ni(II)(DMG)_2$), respectively. As shown in Fig. 1a, there is a broad absorption band around 3,200 cm^{-1} superimposed with a number of weak side bands, which can be attributed to the N–O–H stretching mode. In the spectrum of $Ni(II)(DMG)_2$ as shown in Fig. 1b, this absorption band almost disappeared, suggesting the N–O–H stretching mode becomes very weak after the coordination with Ni(II). This indicates that this bond is significantly weak due to the formation of the Ni–N bond in the complex. A new weak band at 1,790 cm^{-1} indicates a strong intramolecular hydrogen bonding in the $Ni(II)(DMG)_2$ complex [25]. Another characteristic absorption band appears

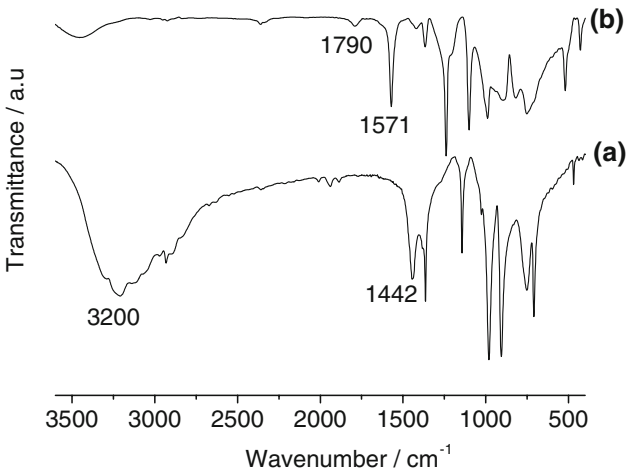

Fig. 1 FTIR spectra of (**a**) dimethylglyoxime molecule and (**b**) bis-(dimethylglyoximato) nickel(II) complex

for DMG at 1,442 cm^{-1}, which can be assigned to the C=N stretching mode. In the spectrum of Ni(II)$(DMG)_2$, this band has shifted to a higher frequency of 1,571 cm^{-1}. This difference may originate from the longer C=N bond length in the Ni(II)$(DMG)_2$ complex due to its covalent characteristics compared with the C=N bond in the precursor DMG [26]. The adsorption band at 1,367 cm^{-1} for DMG, which is due to the bending of the N–OH bond, decreased significantly in Ni$(DMG)_2$. Also, the adsorption band that appears at 1,234 cm^{-1} is due to the stretching mode of the N–O bond of the ionized N–OH group in DMG after coordination with Ni(II). All these features confirmed the formation of Ni$(DMG)_2$ [27–30], and the infrared spectrum of the product shown in Fig. 2 is consistent with the spectrum of the Ni(II)$(DMG)_2$ complex reported in the literature [27–30]. This confirms that the target Ni(II)$(DMG)_2$ complex was successfully synthesized in this work, whose structure has been reported previously [25–27].

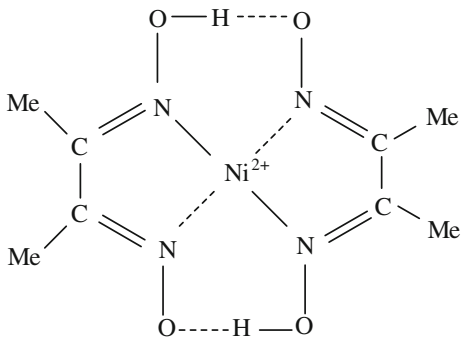

Fig. 2 Molecular structure of bis-(dimethylglyoximato) nickel(II) (Ni(II)$(DMG)_2$) [25–27]

2.2 Electrochemical measurements

A BAS model CV-50 W potentiostat was used in all voltammetric experiments. A three-electrode cell was used for electrochemical measurements; it consisted of a graphite disc (diameter: 0.6 cm) or a carbon paste disk as a working electrode, a platinum wire as an auxiliary electrode, and a saturated Ag/AgCl (in saturated KCl) or saturated calomel electrode (SCE) as the reference electrode. The two reference electrodes were tested in 0.1 M NaOH solution and showed stable electrode potentials within the measurement time scale.

2.3 Preparation of modified electrodes

2.3.1 Modified graphite electrode

Prior to each experiment, the graphite electrode surface was polished with 400-grit sandpaper until a mirror-like surface was obtained. Next, 50 μL of 1×10^{-2} M DMG acetone solution was added to the pretreated electrode surface and allowed to dry in air at room temperature. An aliquot of (5, 10, 15, or 25 μL) of 1×10^{-3} M Ni(II) sulphate aqueous solution was then added on the DMG-coated electrode surface and allowed to dry in air at room temperature. The electrode was then transferred to a 0.1 mol L^{-1} NaOH solution, and activated by successive sweeping between 0 and 0.8 V (versus Ag/AgCl), at a scan rate of 100 mV s^{-1} for 80 cycles.

2.3.2 Modified carbon paste electrode

The carbon paste electrode was prepared by uniformly mixing graphite paste with Ni(II)$(DMG)_2$ at different ratios. A small amount (1 μL) of liquid hydrocarbon was used as a binder in the paste. The electrode end contained a glass cavity with an area of 0.21 cm^2 and a depth of 0.1 cm, in which the catalyst-carbon paste was pressed to form a target electrode surface.

3 Results and discussion

3.1 Electrochemical responses from an Ni-DMG modified graphite electrode surface

Figure 3 shows the cyclic voltammograms (CVs) of a Ni(II)$(DMG)_2$-complex-coated electrode in 0.1 mol L^{-1} NaOH solution. The peak current increases with the scanning, indicating the formation of $[(DMG)_2(H_2O)Ni(III)ONi(III)(OH)(DMG)_2]^-$ film (see below for more discussion) on the electrode surface during the scanning process. The Ni(II)$(DMG)_2$ complex was formed in the process of

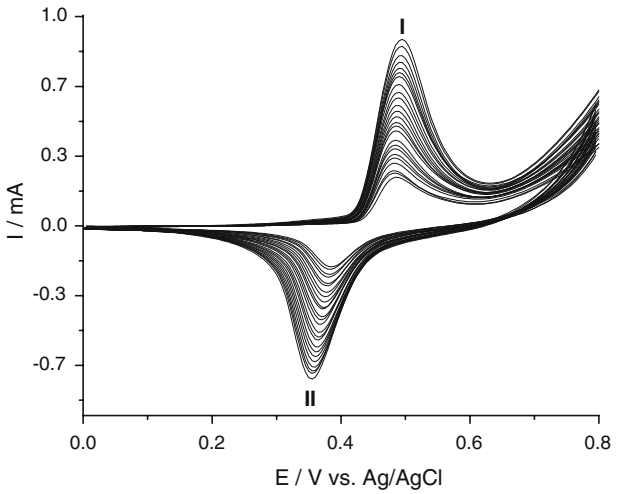

Fig. 3 CVs of Ni(II)$(DMG)_2$ modified graphite electrode in 0.1 M NaOH solution. Scan rate: 100 mV s^{-1} (~80 cycles). Surface Ni(II)$(DMG)_2$ loading: (Γ) 1.51 × 10^{-8} mol cm^{-2}

deposition, and $[(DMG)_2(H_2O)Ni(III)ONi(III)(OH)(DMG)_2]^-$ could have been produced in the potential scanning process.

3.1.1 *Ni(II)$(DMG)_2$ structure after potential cycling*

In order to find how many OH^- are involved in the redox reaction shown in Fig. 3, the surface CVs of the modified electrode formed in the potential scanning process were recorded in 1.0 × 10^{-4}, 1.0 × 10^{-3}, 1.0 × 10^{-2}, 0.1, and 1.0 M NaOH solutions. For NaOH solutions with concentrations less than 0.1 M, NaCl was added to maintain a total electrolyte concentration of 0.1 M. It was reported that the addition of Cl^- does not affect the electrochemical behaviour of the Ni(II) complex [12]. Figure 4 shows the average peak potential (the average of the anodic and cathodic peak potentials) as a function of the solution pH. A linear relationship between the average peak potential and the pH is observed, and a slope of 83 mV/pH is obtained, close to a theoretically expected value of 89 mV/pH for a redox process with 1.5 protons per electron transfer. This result suggests that 1.5 protons per electron transfer are involved in the redox process shown by waves I and II in Fig. 3.

The reactions in the electrode preparation process can be explained as follows. In the deposition process [17, 18], the reaction described by reaction (I) should occur to form a surface complex of Ni(II)$(DMG)_2$. In the potential scanning process [19–21], the reaction can be described as reaction (II),

$$2Ni(II)(CH_3C(=NO)C(=NOH)CH_3)_2 + 3OH^- \rightarrow [CH_3C(=NO)C(=NOH)CH_3)_2(HO)Ni(III) - O - Ni(III)(H_2O)(CH_3C(=NO)C(=NOH)CH_3)_2]^- + 2e^- \quad (II)$$

in which 2 electrons and 3 hydroxide ions are involved. This is consistent with the pH dependency shown in Fig. 4.

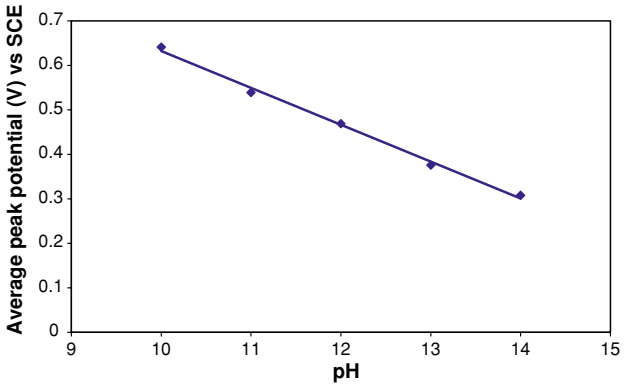

Fig. 4 Average peak potentials of the Ni(II)$(DMG)_2$ redox process as a function of solution pH. Potential scan rate: 50 mV/s

The product is thereafter abbreviated as $[(DMG)_2(H_2O)Ni(III)ONi(III)(OH)(DMG)_2]^-$.

In the literature, the corresponding oxidation of Ni(II)$(DMG)_2$ and other Ni complexes such as nickel-porphyrin on the electrode surface have been explained as reaction (III) [14, 16, 21]:

$$NiO + OH^- \rightarrow NiOOH + e^- \quad (III)$$

This explanation does not consider the coordinating ligands, which causes the misconception that the coordination compounds were dissociated. The coordination compound of $Ni(DMG)_2$ is highly stable with a stability constant of 4 × 10^{-24}, and the dissociation of this compound in an alkaline solution requires high temperatures in hydrothermal conditions [31].

Ni et al. [32] have studied the structure of oxidized Ni(II)$(DMG)_2$ using XPS. They found that in the oxidized form (in solid state form), Ni was Ni(III), and the structure was $Ni(III)[(CH_3C(=NO)C(=NO)CH_3)(CH_3C(=NOH)C(=NO)CH_3)_2]$, where the coordinate number of Ni(III) was still 4. They proposed that in solutions, the oxidized Ni(II)$(DMG)_2$ could form 5 or 6 coordinated compounds. Roslonek and Taraszewska [12] found that OH^- had a strong tendency to coordinate Ni(II) metal centers in a Ni(II)–cyclam complex, and that half of the Ni(II)–cyclam appeared in the octahedral form in 0.1 M NaOH solution. The structure of Ni–cyclam in the solution was proposed to be $Ni(II)(OH)(H_2O)$(cyclam), where the coordinate number of Ni(II) is 6. An oxo group that played a key role in the catalytic activity exists in Ni(III) hydroxide, the structure of which is NiOOH. Roslonek and Taraszewska proposed that on an Ni(II)–cyclam complex modified electrode, oxo-bridges between Ni(III) complexes could be formed through the oxidation of Ni(II) complexes, leading to film growth on the electrode surface [12]. Kotz and Yeager [33] made a similar suggestion for cobalt phthalocyannine oxidation on a silver electrode. The voltammetric response observed here in Fig. 3 is similar to that reported on other Ni(II) complexes such as Ni(II)–cyclam, Ni(II) curcumin,

and polymerized Ni(II) tetrakis(3-methoxy-4-hydroxyphenyl) porphyrin (poly-Ni(II)TMHPP) [12, 15, 22, 23]. Therefore, the formation of an oxo-bridge between two adjacent Ni(III) centers is believed to be a product of $Ni(II)(DMG)_2$ electro-oxidation. The proposed structure of $[(DMG)_2(H_2O)Ni(III)ONi(III)(OH)(DMG)_2]^-$ is shown in Fig. 5.

3.1.2 Cycling potential effect

Scanning the $Ni(II)(DMG)_2$ coated graphite electrode to a high potential is necessary to form $[(DMG)_2(H_2O)Ni(III)ONi(III)(OH)(DMG)_2]^-$. Figure 6 shows the 30th CV scan of $Ni(DMG)_2$ coated graphite electrodes cycling in a 0.1 M NaOH solution in potential ranges of −0.1 to 0.5 V, −0.1 to 0.6 V, −0.1 to 0.7 V, and −0.1 to 0.8 V versus SCE. A freshly polished graphite electrode was used for each experiment. The redox peak current increases as the potential range positively increases, indicating that more $[(DMG)_2(H_2O)Ni(III)ONi(III)(OH)(DMG)_2]^-$ complex is produced. There is almost no distinguishable redox peak when the CV is scanned to 0.5 V. However, a very small peak was observed when it was scanned to 0.6 V, and a medium redox peak was found when it was scanned to 0.7 V. The highest peak current was observed when potential was scanned to 0.8 V.

3.1.3 Graphite surface effect

Figure 7 shows the 30th CV scan of $Ni(II)(DMG)_2$ coated on a pre-polarized graphite electrode in the potential range of −0.1 to 0.5 V (versus SCE). The electrode was held at 0.8 V (versus SCE) for 10 min before coating it with $Ni(II)(DMG)_2$. The redox peak of $[(DMG)_2(H_2O)Ni(III)ONi(III)(OH)(DMG)_2]^-$ could be seen on the $Ni(II)(DMG)_2$ coated pre-polarized graphite electrode. The pre-polarization of the graphite surface resulted in the formation of surface functional groups and

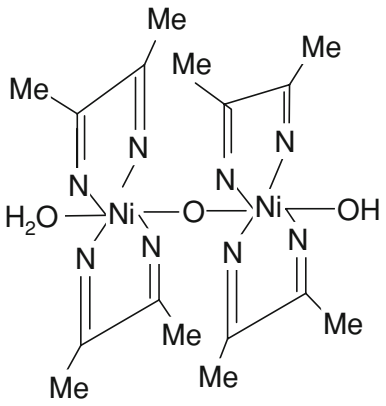

Fig. 5 Proposed molecular structure of $[(DMG)_2(H_2O)Ni(III)O-Ni(III)(OH)(DMG)_2]^-$, Me in the structure represents (CH_3)

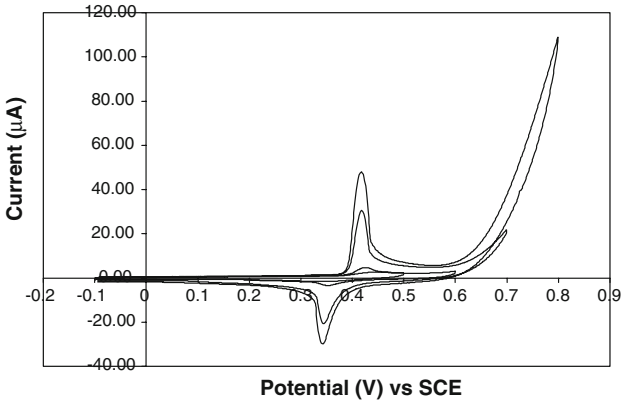

Fig. 6 The 30th scan of CV of $Ni(II)(DMG)_2$ modified graphite electrodes in different potential range (−0.1 to 0.5, 0.6, 0.7, and 0.8 V versus SCE). Potential scan rate: 100 mV/s

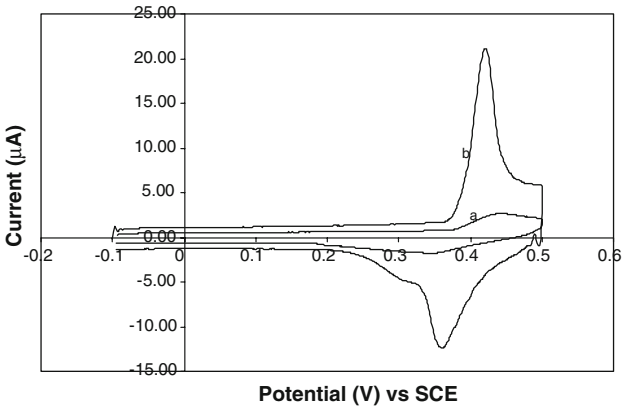

Fig. 7 The 30th scan of CV of $Ni(II)(DMG)_2$ coated on (**a**) a non-polarized (freshly polished) graphite electrode, and (**b**) on a pre-polarized graphite electrode which was held at 0.8 V for 10 min before coated with the catalyst. Scan rate: 100 mV/s

radicals, which facilitated the formation of $[(DMG)_2(H_2O)Ni(III)ONi(III)(OH)(DMG)_2]^-$. For comparison, the curve was also measured in the same potential range but the electrode had not been held at any potential before coating it with $Ni(II)(DMG)_2$. On the non-polarized surface, there were few functional groups and radicals. Therefore, $[(DMG)_2(H_2O)Ni(III)ONi(III)(OH)(DMG)_2]^-$ could not be produced. More work is necessary to determine the formation mechanism.

3.1.4 Surface concentration of the $Ni(II)(DMG)_2$ complex

Assuming that all the films formed on the electrode surface are electroactive, the surface concentration can be calculated according to Eq. 1,

$$\Gamma = Q/nFA \quad (1)$$

where Γ is the surface concentration of $[(DMG)_2(H_2O)Ni(III)ONi(III)(OH)(DMG)_2]^-$ in mol cm^{-2}, Q is the charge under the oxidation peak (I_{pa}) for the voltammogram recorded in 0.1 mol L^{-1} NaOH, A is the geometric surface area of

the graphite electrode, and n is the electron number transferred in the redox reaction, which is 1 per nickel.

The surface concentrations of the Ni(II)$(DMG)_2$ complex were calculated to be 7.57×10^{-9}, 1.51×10^{-8}, 2.27×10^{-8}, and 3.78×10^{-8} mol cm^{-2}, respectively, for the aliquot of 5, 10, 15, and 25 μL Ni (II) solutions used. The surface concentration increases linearly with the increase in the amount of Ni(II) added.

3.1.5 *Potential scan rate dependency of the peak currents*

The surface CVs were recorded at various scan rates in 0.10 mol L^{-1} NaOH solution. It was observed that the peak current did not increase linearly with an increase in the square root of the potential scan rate, as shown in Fig. 8. Rather, a linear relationship of I_p versus v was observed. These features suggest that the electrochemical process of reaction (II), within the film, follows thin layer behaviour.

3.2 Ni(II)$(DMG)_2$ modified carbon paste electrode

CV and a plot of peak current versus square root of scan rate obtained with a Ni(II)$(DMG)_2$ carbon paste electrode (not shown) are different from that obtained with the modified graphite electrode. A linear relationship was observed, suggesting that the redox process of the $[(DMG)_2(H_2O)Ni(III)ONi(III)(OH)(DMG)_2]^-$ complex within the carbon paste layer is a diffusion process. This process could be related to counter-anion diffusion into and out of the modified electrode during the oxidation and reduction processes [8, 16]. This is reasonable, as in a carbon paste electrode, some of the catalyst is buried deep in the electrode, and diffusion of the counter anion to all the catalyst is more difficult than on a modified graphite surface electrode.

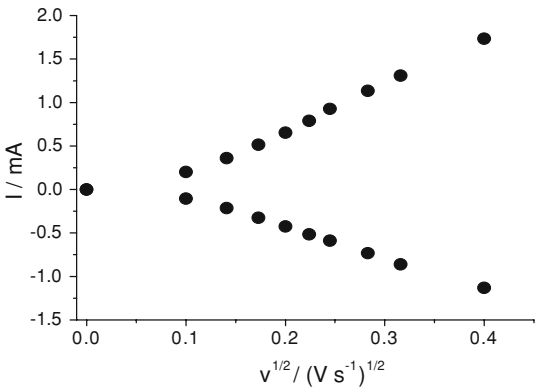

Fig. 8 Plots of anodic and cathodic peak currents versus the square root of potential scan rate. Data was taken from the CVs of a Ni(II)$(DMG)_2$ modified graphite electrode in a 0.1 mol L^{-1} NaOH solution with potential scan rates of 10, 20, 30, 40, 50, 60, 80 and 160 mV s^{-1}. Surface Ni(II)$(DMG)_2$ loading: $\Gamma = 1.51 \times 10^{-8}$ mol cm^{-2}

3.3 Electrocatalytic activity of Ni(II)$(DMG)_2$ modified carbon paste electrode towards methanol and ethanol oxidation

3.3.1 *Cyclic voltammograms*

Figure 9a and b shows the CVs of catalyzed methanol and ethanol oxidation, respectively, on a Ni(II)$(DMG)_2$ complex modified carbon paste electrode. For comparison, the CVs in the absence of alcohol on the same electrode are also plotted in the same figure. The alcohol oxidation currents starting from ~0.25 V clearly demonstrate that the $[(DMG)_2(H_2O)Ni(III)ONi(III)(OH)(DMG)_2]^-$ modified electrode shows catalytic activity toward both methanol and ethanol oxidation. The onset potentials for both methanol and ethanol oxidation are very close to that of Ni(II)$(DMG)_2$ oxidation, indicating that the oxidation product of Ni(II)$(DMG)_2$, which is $[(DMG)_2(H_2O)Ni(III)ONi(III)(OH)(DMG)_2]^-$, should be responsible for the catalytic activity. The shape of the oxidation CVs in Fig. 8 are similar to those reported for electrocatalytic alcohol oxidation [21, 34].

3.3.2 *Catalyst loading effect*

Ni(II)$(DMG)_2$ loading in the carbon paste layer represents the concentration of the catalyst active site. Increasing the loading should affect the catalytic current of the alcohol oxidation. To examine this effect, four separate carbon paste layers containing 2.5, 5.0, 10.0, and 20.0 (wt%) of Ni(II)$(DMG)_2$ with respect to moles of carbon were prepared. The results obtained in a 1.0 mol L^{-1} NaOH + 0.3 mol L^{-1} methanol solution are plotted in Fig. 10. A monotonic increase in the peak current of methanol electrocatalytic oxidation with increasing Ni(II)$(DMG)_2$ loading can be observed, as shown in the inset of Fig. 10. For ethanol, similar behavior was observed. However, the results show that the oxidation current reaches a plateau after the Ni(II)$(DMG)_2$ loading becomes larger than 10%, as shown in the insert of Fig. 10. This may be due to diffusion limitations of either methanol or OH^- to the electrode. As the catalyst loading increased, more catalyst was buried inside the electrode, and diffusion of reactants to these catalytic sites becomes more challenging.

3.3.3 *OH^- concentration effect*

It is expected that the concentration of OH^- ions in the electrolyte solution should play a role in the catalytic oxidation of both methanol and ethanol. Thermodynamically, an increase in OH^- concentration should cause a shift in the alcohol oxidation potential to more negative values. Figure 11 shows the catalytic oxidation of ethanol in three solutions containing 0.1, 0.5, and 1.0 mol L^{-1} of

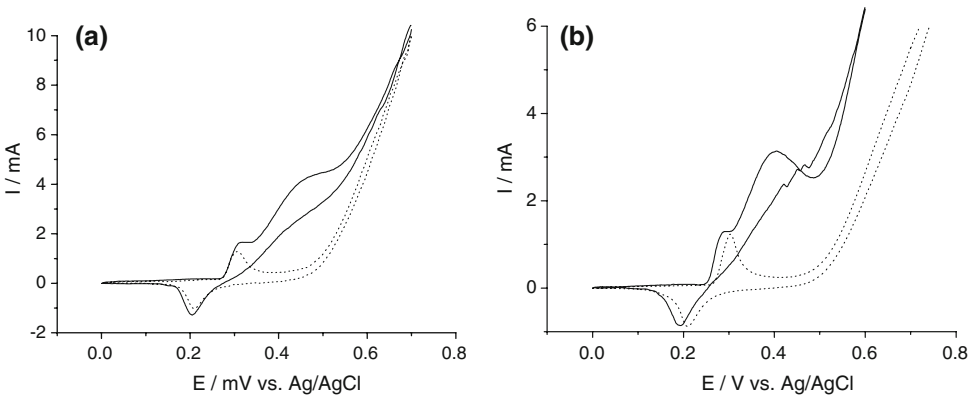

Fig. 9 CVs for Ni(II)(DMG)$_2$ complex in 1.0 mol L^{-1} NaOH in the absence (- - -) and presence (—) of 0.1 mol L^{-1} of alcohol. (**a**) Methanol and (**b**) ethanol. Potential scan rate: 5 mV s^{-1}. Loading of Ni(II)(DMG)$_2$: 10 wt%

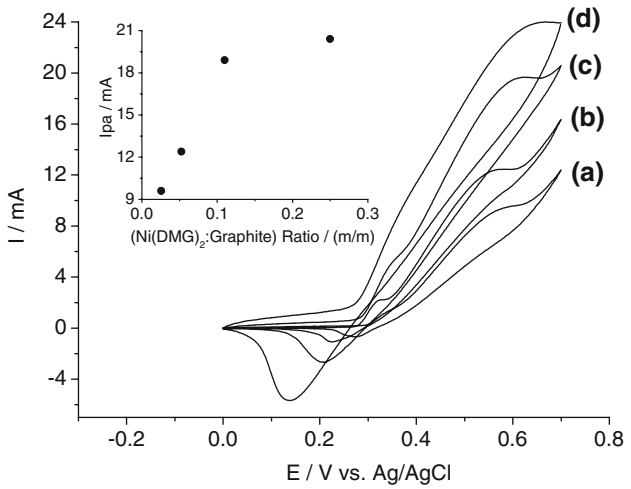

Fig. 10 CVs of carbon paste electrodes loaded by different quantities of Ni(II)(DMG)$_2$: (**a**) 0.5%, (**b**) 5.0%, (**c**) 10.0%, and (**d**) 20.0 (wt%) of Ni(II)(DMG)$_2$. Testing solution: 1.0 mol L^{-1} NaOH + 0.3 mol L^{-1} methanol. Potential scan rate: 0.01 V s^{-1}. Inserted figure: Effect of the catalyst loading on the peak current of methanol oxidation

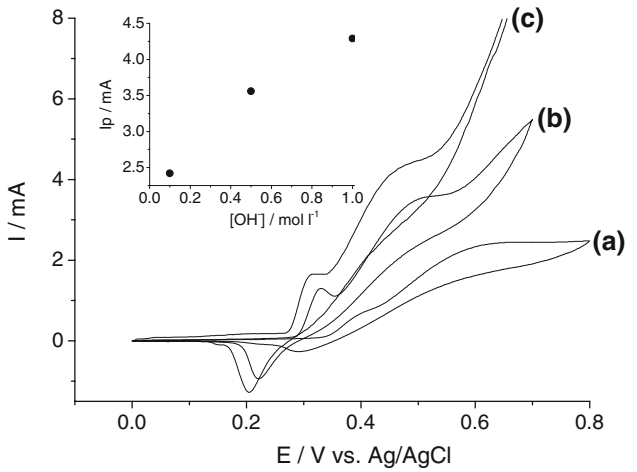

Fig. 11 CVs of a carbon paste electrode modified by Ni(II)(DMG)$_2$ in solutions containing (**a**) 0.1, (**b**) 0.5, and (**c**) 1.0 mol L^{-1} of NaOH, respectively. Methanol concentration in each solution was 0.1 mol L^{-1}. Inserted figure: Effect of OH$^-$ concentration on the peak current of methanol oxidation. Potential can rate: 0.005 V s^{-1}. Loading of Ni(II)(DMG)$_2$: 10 wt%

NaOH. A negative shift in peak potential can be observed when the OH$^-$ concentration is changed from 0.1 to 1.0 mol L^{-1}, as shown in the insert of Fig. 11. However, the catalytic current of the alcohol oxidation also increases with increasing OH$^-$ concentration, indicating that the OH$^-$ ion participates in the oxidation. Therefore, the proposed reaction mechanism should reflect this OH$^-$ participation (see below).

3.3.4 Potential scan rate effect

CVs for the catalytic oxidation of both methanol and ethanol on a carbon paste electrode modified by Ni(II)(DMG)$_2$ were also recorded at different potential scan rates. The current peaks of both methanol and ethanol oxidation increased linearly with the square root of the scan rate, suggesting a reactant diffusion-controlled process [35].

3.3.5 Alcohol concentration effect

The effect of methanol (or ethanol) concentration on the CV peak current and the peak potential of a Ni(II)(DMG)$_2$ modified carbon paste electrode were also investigated in a solution of 1.0 mol L^{-1} NaOH. The results are shown in Fig. 12. It can be seen that in Fig. 12a the peak current for the catalytic oxidation of both alcohols increases with increasing concentration. Linear relationships between the CV peak current and the reactant concentration for both methanol and ethanol can be observed in the concentration range of 0–0.5 mol L^{-1}. In Fig. 12b, it can be also observed that the peak potentials for both alcohols shift positively with increasing alcohol concentration. These results suggest that the catalytic oxidation of both alcohols is controlled by the diffusion of the reactant. The consistent increase in the oxidation peak currents of both methanol and ethanol with reactant concentration, shown in Fig. 12b, could be employed in the analysis of alcohol concentration.

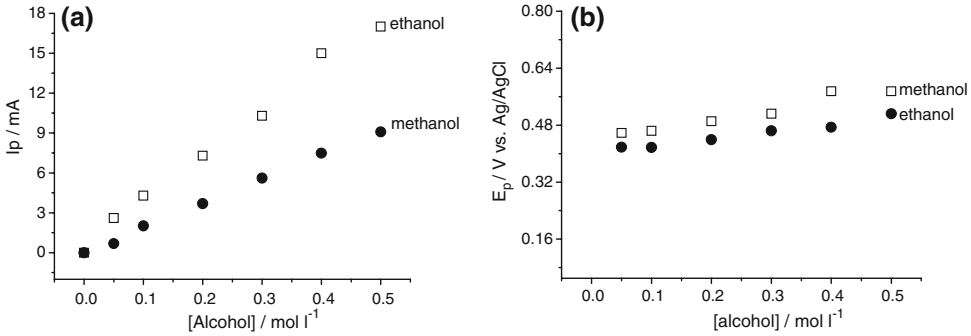

Fig. 12 (**a**) Peak currents and (**b**) peak potentials of methanol and ethanol catalytic oxidation as a function of alcohol concentration. Carbon paste electrode modified with 10 wt% of $Ni(II)(DMG)_2$. CVs recorded in 1.0 mol L^{-1} of NaOH with a potential scan rate of 0.005 V s^{-1}

Therefore, the carbon paste electrode modified by the $Ni(II)(DMG)_2$ complex might be able to serve as a sensor probe for methanol and ethanol analysis.

At very low OH^- concentrations, the alcohol oxidation current did not increase linearly with alcohol concentration. For example, Fig. 13 shows the dependency of the oxidation peak current on methanol concentration at different OH^- concentrations. In 1.0 M NaOH solution containing methanol, methanol oxidation current increases linearly with methanol concentration in the range of 0–0.5 M; in 0.5 M NaOH solution containing methanol, the oxidation current-methanol concentration relationship became a curve with a plateau after methanol concentration is larger than 0.4 M, and in 0.1 M NaOH solution containing methanol, the oxidation current remained unchanged after methanol concentration is larger than 0.1 M. These results strongly suggest that the OH^- ion plays an important role in the catalytic oxidation of both methanol and ethanol, and that the alcohol oxidation is diffusion limited in these solutions. The literature has also shown this behavior for methanol and ethanol electrooxidation in a basic medium on a nickel oxide electrode, which was explained by the direct participation of the OH^- ion in the oxidation process [18, 21].

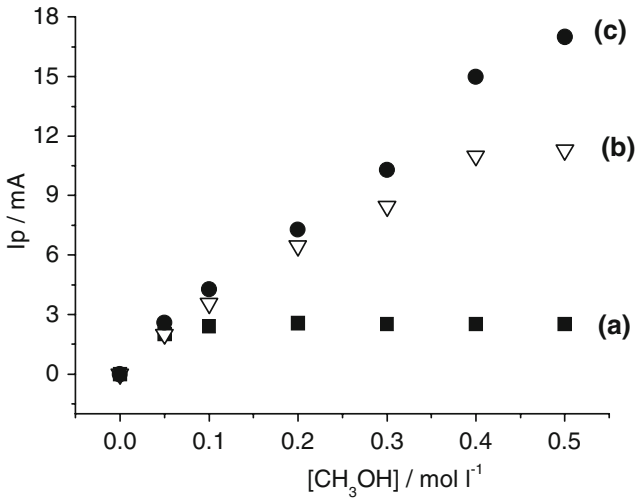

Fig. 13 Peak currents of methanol concentration range 0.1 to 0.5 mol L^{-1} as a function of different OH^- concentrations (mol L^{-1}): (**a**) 0.1, (**b**) 0.5, and (**c**) 1.0. Carbon paste electrode modified with 10 wt% of $Ni(II)(DMG)_2$. CVs recorded with a potential scan rate of 0.005 V s^{-1}

3.4 Discussion of the mechanism of electrocatalytic oxidation of both methanol and ethanol

It is generally agreed that the Ni-based catalysts such as nickel oxides and complexes in a basic aqueous medium can catalyze methanol and ethanol oxidation through an overall four-electron process producing formate anion (methanol oxidation) and acetate anion (ethanol oxidation):

$$CH_3OH + 5OH^- \rightarrow HCOO^- + 4H_2O + 4e^- \text{(methanoloxidation)} \quad \text{(IV)}$$

$$CH_3CH_2OH + 5OH^- \rightarrow CH_3COO^- + 4H_2O + 4e^- \text{(ethanoloxidation)} \quad \text{(V)}$$

In order to confirm this four-electron process, experiments with a $[(DMG)_2(H_2O)Ni(III)ONi(III)(OH)(DMG)_2]^-$ coated graphite rotating disk electrode (RDE) were carried out in a 1.0 mol L^{-1} NaOH solution containing either 0.1 mol L^{-1} of ethanol or 0.1 mol L^{-1} of methanol. Theoretically, RDE is accurate with a smooth electrode, rather than with a rough or film coated surface. However, if the surface roughness is much lower than the diffusion layer thickness, this method may be a good approximation for the reaction kinetic estimation. The curves of the current density versus electrode potential were recorded at different electrode rotation rates. According to rotating disk electrode theory [35], the current density (i) at each electrode potential (E) should contain two contributions, one from the kinetics current density (i_k) and the other from the diffusion current density (i_d). The relationship among these three current densities can be expressed as Eq. 2:

$$i_k = i\left(\frac{i_d}{i_d - i}\right) \quad (2)$$

According to the Koutecky–Levich theory [35], the diffusion current density in Eq. 2 can be expressed as Eq. 3,

$$i_d = 0.62nFACD^{2/3}v^{-1/6}\omega^{1/2} \quad (3)$$

where ω is the rotation rate of the disk electrode, n is the number of transferred electrons in the overall reduction process, F is the Faraday constant, C is the concentration of ethanol (or methanol), D is the diffusion coefficient of the ethanol (or methanol), and v is the kinematic viscosity. Figure 14 shows the Koutecky–Levich plots for ethanol oxidation in 1.0 mol L^{-1} NaOH solution. The theoretical plot for a four-electron transfer process of ethanol oxidation is also shown. The slope of the experimental line, which is similar to that of the 4-electron theoretical line, confirms that a 4-electron oxidation process was achieved.

With respect to the fact that catalyst loading, OH^- concentration, and alcohol concentration have strong effects on the catalytic currents for both ethanol and methanol oxidation, the following mechanism is proposed by referring to the literature [20, 21, 33, 36]:

$$2[Ni(II)(DMG)_2] + 3OH^- \rightarrow [(DMG)_2(H_2O)Ni(III)ONi(III)(OH)(DMG)_2]^- + 2e^- \quad (VI)$$

$$CH_3CH_2OH + OH^- + [(DMG)_2(H_2O)Ni(III)ONi(III)(OH)(DMG)_2]^- \rightarrow [Ni(III)(OH)(DMG)_2(CH_3CH_2O)]^- + [Ni(III)(OH)(DMG)_2(OH)]^- + H_2O \quad (VII)$$

$$CH_3CH_2OH + [Ni(III)(OH)(DMG)_2(OH)]^- \rightarrow [Ni(III)(OH)(DMG)_2(CH_3CH_2O)^-] + H_2O \quad (VIII)$$

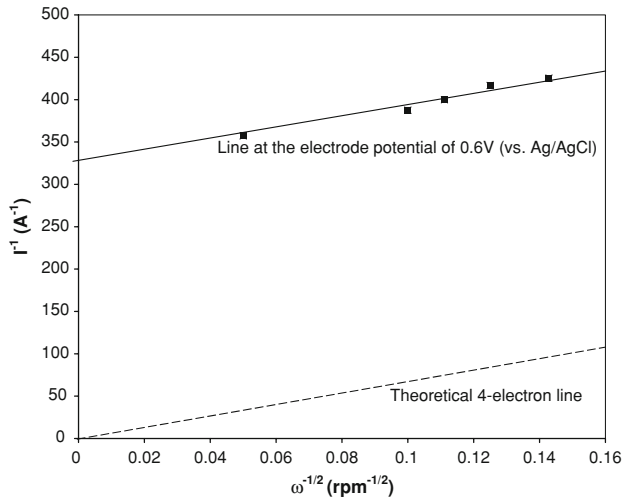

Fig. 14 Koutecky–Levich plots obtained on a rotating graphite disk electrode coated with Ni(II)$(DMG)_2$ catalyst in the presence of 0.1 M of ethanol. Supporting electrolyte: 1.0 mol L^{-1} NaOH. Dashed line is calculated according to the Levich diffusion equation, and the solid point line is that which is measured. The point values were taken at 0.6 V (versus Ag/AgCl) on the current–potential curves

$$[Ni(III)(OH)(CH_3CH_2O)(DMG)_2]^- + OH^- \rightarrow Ni(III)(OH)(CH_3CHO)(DMG)_2 + 2e^- + H_2O \quad (IX)$$

$$Ni(III)(OH)(CH_3CHO)(DMG)_2 + 2OH^- \rightarrow Ni(II)(DMG)_2 + CH_3COO^- + 2H_2O + 2e^- \quad (X)$$

The Ni(II)$(DMG)_2$ formed in reaction (X) will be oxidized back to $[(DMG)_2(H_2O)Ni(III)ONi(III)(OH)(DMG)_2]^-$ according to reaction (VI) continuing the catalytic reaction cycle between reactions (VI) and (X). In this reaction cycle, the total number of electrons involved is 4, resulting in a reaction product of CH_3COO^-. Results in Figs. 10, 11, and 12 show that the catalytic currents monotonically increase with an increase in Ni(II)$(DMG)_2$ catalyst loading, OH^- concentration, and alcohol concentration, suggesting that these three species participate in the rate-determining step in the whole mechanism of alcohol oxidation. Therefore, the most likely rate-determining step could be reaction (VII). It is believed that the reaction mechanism represented by reactions (VI)–(X) for ethanol is also applicable to methanol.

This mechanism is based on our current understanding and literature; it does not necessarily reflect the whole situation. More delicate work is needed for a deeper understanding. The purpose of putting forward this mechanism is to facilitate further discussion and understanding.

4 Conclusions

The Ni(II)$(DMG)_2$ complex modified carbon paste electrode and graphite electrode were prepared. Scanning the electrode to a certain positive potential is required for the formation of $[(DMG)_2(H_2O)Ni(III)ONi(III)(OH)(DMG)_2]^-$. The redox process was identified as a one-electron process from Ni(II)$(DMG)_2$ to $[(DMG)_2(H_2O)Ni(III)ONi(III)(OH)(DMG)_2]^-$, which showed strong catalytic activity towards the electrooxidation of ethanol and methanol. The catalytic oxidation currents consistently increased with increasing Ni(II)$(DMG)_2$ catalyst loading, OH^- concentration, and alcohol concentration.

Based on results that generally agree with those in the literature, we believe this Ni(II)$(DMG)_2$-based catalyst in a basic aqueous medium could catalyze methanol and ethanol oxidation through an overall four-electron process to produce formate anion (methanol oxidation) and acetate anion (ethanol oxidation). This four-electron process was confirmed by results obtained with a $[(DMG)_2(H_2O)$-$Ni(III)ONi(III)(OH)(DMG)_2]^-$ coated graphite rotating disk electrode in a 1.0 mol L^{-1} NaOH solution containing either 0.1 mol L^{-1} of ethanol or 0.1 mol L^{-1} of methanol. The slope of experimental Koutecky–Levich plot was the

same with that of the theoretical one calculated under the same conditions.

Acknowledgements The authors are grateful for the support of CNPq (Project ETACOMB, Proc. 505167/2004-2) and PETROBRAS, Brazil, and the Institute for Fuel Cell Innovation, National Research Council of Canada.

References

1. Liu H, Song C, Zhang L, Zhang J, Wang H, Wilkinson DP (2006) J Power Sources 155:95
2. Antolini E (2007) J Power Sources 170:1
3. Spendelow JS, Wieckowski A (2007) Phys Chem Chem Phys 9:2654
4. Wang H, Xu C, Cheng F, Jiang S (2007) Electrochem Commun 9:1212
5. Cao L, Sun G, Li H, Xin Q (2007) Electrochem Commun 9:2541
6. Xu C, Hu Y, Rong J, Jiang S (2007) Electrochem Commun 9:2009
7. Gupta SS, Data J (2005) J Power Sources 145:124
8. Taraszewska J, Roslonek G (1994) J Electroanal Chem 364:209
9. El-Shafei AA (1999) J Electroanal Chem 471:89
10. Fleischmann M, Korinek K, Pletcher D (1971) J Electroanal Chem 31:39
11. Casella IG, Cataldi TRI, Salvi AM, Desimoni E (1993) Anal Chem 65:3143
12. Roslonek G, Taraszewska J (1992) J Electroanal Chem 325:285
13. Bae ZU, Park JH, Lee SH, Chang HY (1999) J Electroanal Chem 468:85
14. Golabi SM, Nozad A (2004) Electroanalysis 16:199
15. Ciszewski A, Milczarek G (1997) J Electroanal Chem 426:125
16. Golikand AN, Maragheh MG, Irannejad L, Asgari M (2006) Russ J Electrochem 42:167
17. Flora CJ, Nieboer E (1980) Anal Chem 52:1013
18. Pihlar B, Valenta P, Nurnberg HW (1986) J Electroanal Chem 214:157
19. Korolczuk M (2000) Talanta 53:679
20. Golikand AN, Asgari M, Maragheh MG, Shahrokhian S (2006) J Electroanal Chem 588:155
21. Golikand AN, Shahrokhian S, Asgari M, Maragheh MG, Irannejad L, Khanchi A (2005) J Power Sources 144:21
22. Ciszewski A, Milczarek G (1996) J Electroanal Chem 413:137
23. Malinski T, Ciszewski A, Benett J, Fish JR, Czuchajowski L (1991) J Electrochem Soc 138:2008
24. Malati MA (1999) Experimental inorganic physical chemistry, harwood series in chemical science. Harwood Publishing, Chichester, p 214
25. Ponnuswamy T, Chyan O (2002) Anal Sci 18:449
26. Xavier KO, Chacko J, Yussuf KKM (2004) Appl Catal A 258:251
27. Szabo A, Kovacs A (2003) J Mol Struct 651–653:615
28. Nayak SC, Das PK, Sahoo KK (2003) Chem Pap 57:91
29. Nakamoto K (1970) Infrared spectra of inorganic and coordination compounds. Wiley, New York, p 230
30. Bellamy LJ (1968) Advances in infrared group frequencies. Methuen, London, p 105
31. Young VY, Chang FC, Cheng KL (1987) Appl Spectrosc 41:994
32. Ni X, Zhao Q, Zhang Y, Song J, Zheng H, Yang K (2006) Solid State Sci 8:1312
33. Kotz R, Yeager E (1979) J Electroanal Chem 113:113
34. Pereira MG, Jiménez MD, Elizalde MP, Manzo-Robledo A, Alonso-Vante N (2004) Electrochim Acta 49:3917
35. Bard AJ, Faulkner LR (2001) Electrochemical methods, fundamentals and applications. Wiley, New York
36. Kim JW, Park SM (2005) J Korean Electrochem Soc 8:117